J. Appl. Geodesy, Vol. **7** (2013), pp. 103–113 DOI 10.1515/jag-2013-0053

Automatic optimization of height network configurations for detection of surface deformations

Christoph Holst,[1,*] **Christian Eling**[1] **and Heiner Kuhlmann**[1]

[1] Institute of Geodesy and Geoinformation, University of Bonn, Germany

Abstract. Levellings are performed to observe height changes of different epochs at discrete surveying points. A reliable estimation of surface deformations by a bivariate polynomial needs a sufficient configuration of the underlying network. Because the spacial distribution of the surveying points is not homogeneous in the discussed regions, the network configuration has to be optimized. This study proposes an optimization procedure that estimates the optimal number and position of the surveying points considered for a reliable analysis. Furthermore, the already existing observations are accepted or rejected due to the network's geometry. Therefore, two different approaches are combined. First, the sampling theorem from time series analysis is used to estimate the number and position of the surveying points. Second, the partial redundancies from statistics take the reliability into account. Applying the optimization procedure to several test regions, the benefit of the optimized network configurations is discussed.

Keywords. network optimization, bivariate polynomial, reliability, sampling theorem, partial redundancies, surface deformation.

1 Introduction and background

For the mining of lignite, an extensive dewatering is necessary because of the depth of the opencast coal mines. This causes a subsidence of ground that has to be analyzed and monitored. Therefore, the general purpose of this project is the parameterization of surface deformations by bivariate polynomials based upon levellings at discrete surveying points.

Levellings are performed at bench marks usually fixed to house walls. Height changes of the ground can be calculated at these discrete surveying points by building the difference between the heights of two epochs. Figure 1 shows the positions of the $n = 194$ surveying points of Sample Region A. The corresponding height differences between epochs 1 – 3 (15 year period) are also visualized by different colours.

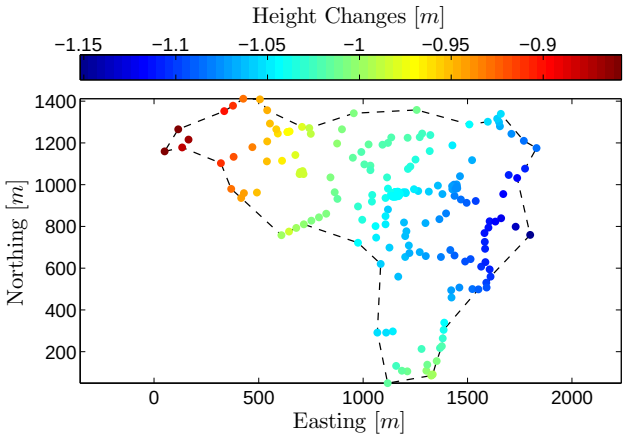

Figure 1. Point cloud and height changes of Region A (epochs 1 – 3, 15 years).

Figure 1 displays that the surveying points are not distributed homogeneously so that the point density varies over different regions. Point aggregations correspond to dense housing, whereas the points with a line structure correspond to courses of streets. However, surface parameterizations generally expect a homogeneous spatial point distribution. An analysis of the height changes in the whole region with optimal reliability is questionable upon these circumstances because of two main aspects:

- Sections with a high point density influence the parameter estimation by a high weight. In contrast, the ones with a low point density do not contribute that much.
- The reliability of the parameter estimation can be insufficient in sections where the point density is too low.

In conclusion, the network configuration should be analyzed and possibly optimized.

This study presents an algorithm that automatically adds new surveying points at positions where they are needed. Moreover, some existing surveying points are rejected due to redundancy. Hence, the algorithm estimates the optimal number and position of surveying points of an existing network.

Corresponding author: Christoph Holst, Institute of Geodesy and Geoinformation, University of Bonn, Nußallee 17, 53115, Bonn, Germany. E-mail: c.holst@igg.uni-bonn.de.

Received: November 08, 2012. Accepted: January 12, 2013.

1.1 Analysis of network configurations

To describe the quality of an existing network configuration, relevant parameters are the ones modelling the influence of each observation on the values of interest. Values of interest could be the estimated parameters or the estimated observations. This correlates highly with the general detection of influential observations in linear regression [5, 10, 18]. For describing observations with high impact, several parameters exist [2]. They can be grouped into the ones being estimated iteratively by empirical simulations and the ones that calculate the impact analytically.

Common parameters used in linear regression are the Cook's Distance [3, 4], the criterion by Pena [22] or the impact factors [31]. These can be assigned to the quality assessment of geodetic networks. While the first two parameters are estimated empirically (first group), impact factors are calculated analytically (second group).

The named parameters of the first group have a high potential to detect high leverage outliers [3]. The criterion by Pena even seems to be able to detect a group of high leverage outliers which can be essential for many applications [22]. Nevertheless, as outliers are excluded before the analysis of the configuration in this study (see Section 2), these parameters are not applicable for the present application.

Impact factors are more suitable for this application [28]. They detect observations with high influence simply by the geometry of the network without using the actual observations [6, 27, 31]. They are introduced in Subsection 3.2.

1.2 Optimization of network configurations

The design stage of geodetic networks is separated in four different orders. The zero, first and second order design are concerned with the installation of a new network. Here, the choice of datum (zero order), configuration (first order) and the weight of individual observations (second order) is established [23, 26]. In contrast, the third order design optimally improves an existing network [26]. This improvement is necessary if parts of the network turn out to be weak concerning the user's requirements [24]. The present study optimizes the configuration of a given height network. Thus, it is part of the third order design.

The third order design optimizes the reliability (i.e. the configuration) as well as the precision (i.e. the individual weights of the observations). In planar networks, this usually leads to the modification of the observation plan, the precision and weights of the observations, respectively [11]. Additional distance or angle measurements between already existing stations are integrated [28], criterion matrices are introduced [7] or shift-vectors are estimated [14].

These aspects are not considered in the present study because the method of measurement (levelling) and its precision are given. Rather an optimization of the geometry, i.e. a densification and a thinning, is necessary to increase the reliability of the parameter estimation. This is also discribed in the literature where the insertion of additional stations [26] or the optimal positioning of given observations [16] are mentioned. Unfortunately, none of these third order designs are able to determine the optimal number of additional observations or surveying points, respectively, as well as to position them at new stations where they are needed most.

The purpose of applied network design is not to optimize the reliability or the precision to inifite magnitude. Rather, it is the optimization of these criterions under the ascpect of economy [13]. Optimization means thus an improvement of the existing network until it becomes economic, reliable and accurate enough [26]. Thereby, the economy is often integrated by a threshold that indicates the maximum precision or reliability that should be achieved. Higher values are then not desired.

1.3 Main aspects of this study

In this study, a third order design strategy is presented. This strategy analyzes and optimizes – if necessary – the configuration of a given height network. This optimization is dependent on the complexity of the modelled height changes. The optimized point cloud is then suitable to reliably estimate surface deformations. Accordingly, the main aspects are the recommodations

- where new surveying points should be positioned (to raise the reliability) and
- also where the point density can be reduced (to raise the cost effectiveness).

Two different approaches are merged in this strategy: First, the sampling theorem used in time series analysis. This estimates the optimal number and position of the surveying points. Second, the partial redundancies known in statistics and linear regression. They verify the reliability of the optimized configuration.

Section 2 presents the measurement and adjustment procedure for the estimation of the bivariate polynomial. Section 3 shows the new developed optimization procedure and Section 4 verifies this strategy.

2 Detection of surface deformations

Levellings are used for the detection of surface deformations. By building the difference between the levellings of different epochs, height changes can be analyzed at discrete surveying points. To describe the height changes continuously, they are approximated by an adapted model. This is developed in a stepwise adjustment procedure. The following subsections explain the fundamentals of this procedure.

2.1 Measurement of height changes

Height changes $\Delta height_i$, with $i = 1, ...n$ representing the number of surveying points, are received by substracting the height of two epochs 2 and 1 at one surveying point i: $\Delta height_i = height_i^{(2)} - height_i^{(1)}$. These heights $height_i$ are gained by a pre-adjustment of the levellings within each epoch. Notwithstanding the fact that the height changes are therefore the outcome of a preprocessing, they are in the following considered as observations $l_i = \Delta height_i$. These observations $\mathbf{l} = [l_1, ..., l_n]^T$ are the basis of further investigations.

By performing a geodetic high precision levelling, an accuracy for the height changes between two epochs of $\sigma = 1mm$ can be reached. In this value, the measurement accuracy as well as the quality of the point definition is included. This magnitude can be confirmed by empirical investigations as well as by the long-time experience of practical surveyors [34].

2.2 Parameterization of surface deformations

For parameterization of the height changes, a bivariate polynomial is chosen. Polynomials enable an approximation of the height changes with globally defined parameters. From the view of approximation, especially splines among other parameterizations could be appropriate as well. Splines being defined locally in a fitnite grid [9] are often used in other studies of comparable application [21, 33]. The differences between the approximation results of polynomials and splines concerning the number of parameters or the smoothness of the derived surface deformations can be insignificant as well as enormous. This depends i.a. on the finite grid of the splines or their basis functions.

Disregarding these facts, the selection of bivariate polynomials is not based on the view of approximation. Rather, it is the aim to determine the global complexity of the surface height changes, i.e. the included waves and their smoothness. Here, polynomials seem to be more appropriate because the smoothness, complexity and the included waves result straightforward from the parameters and their number (see Subsections 2.4 and 3.3.1).

Nevertheless, polynomials cannot approximate height changes of arbitrary complexity. Regions with bounded anomalies, fold lines or other local abnormalities cannot be covered straightforward by bivariate polynomials.

In general, a bivariate polynomial P of order a in both planar directions is defined as [17]

$$P(x_i, y_i) = \sum_{k=0}^{a} \sum_{m=0}^{a-k} p_{k,m} x_i^k y_i^m. \tag{1}$$

The number of surveying points is $i = 1, ..., n$, the planar coordinates of the bench marks where the height changes are observed are x_i, y_i and $\mathbf{p} = [p_{0,0}, p_{0,1}, ..., p_{a,0}]^T$ are the parameters. The maximal number $u_{\max}$ of parameters corresponding to a defined order a can be calculated by [17]

$$u_{\max} = \frac{(a+1)(a+2)}{2}. \tag{2}$$

2.3 Least squares parameter estimation

The parameters $\mathbf{p}$ of the bivariate polynomial are estimated within a classical least squares approch, i.e. the Gauß-Markov model. The functional model is defined as [15]

$$\mathbf{l} + \mathbf{v} = \mathbf{A}\mathbf{p}. \tag{3}$$

The vector of residuals equals $\mathbf{v}$ and the design matrix $\mathbf{A}$ consists of the partial derivatives of the bivariate polynomial of eq. (1) with respect to the parameters $p_{k,m}$. The associated stochastic model, i.e. the covariance matrix $\mathbf{\Sigma}_{ll}$, is

$$\mathbf{\Sigma}_{ll} = \sigma^2 \mathbf{Q}_{ll} = \sigma^2 \mathbf{I} \tag{4}$$

where $\mathbf{I}$ equals the identity matrix and $\mathbf{Q}_{ll}$ the cofactor matrix. Here, correlations are neglected, the observations have identical weights and measurement errors are aussumed to be Gaußian distributed. By minimizing the cost function $\mathbf{v}\mathbf{\Sigma}_{ll}^{-1}\mathbf{v}^T$, the least squares solution of the parameters $\hat{\mathbf{p}}$ and its corresponding covariance matrix $\mathbf{\Sigma}_{\hat{p}\hat{p}}$ are gained

$$\hat{\mathbf{p}} = \left(\mathbf{A}^T \mathbf{Q}_{ll}^{-1} \mathbf{A}\right)^{-1} \mathbf{A}^T \mathbf{Q}_{ll}^{-1} \mathbf{l} \tag{5}$$

$$\mathbf{\Sigma}_{\hat{p}\hat{p}} = \sigma^2 \cdot \left(\mathbf{A}^T \mathbf{Q}_{ll}^{-1} \mathbf{A}\right)^{-1}. \tag{6}$$

The estimated residuals $\hat{\mathbf{v}}$ that should underly a normal distribution are then calculated by

$$\hat{\mathbf{v}} = \mathbf{A}\hat{\mathbf{p}} - \mathbf{l}. \tag{7}$$

The a posteriori standard deviation $\hat{s}$ is given by

$$\hat{s} = \sqrt{\frac{\hat{\mathbf{v}}^T \mathbf{Q}_{ll}^{-1} \hat{\mathbf{v}}}{r}} \tag{8}$$

where r is the redundancy

$$r = n - u. \tag{9}$$

The global test proofs the consistence between a priori variance σ^2 and a posteriori variance $\hat{s}^2$ [19]

$$H_0 : \begin{cases} \hat{s}^2/\sigma^2 < f_{\alpha,r,\infty} & \text{if } \hat{s}^2 > \sigma^2 \\ \sigma^2/\hat{s}^2 < f_{\alpha,\infty,r} & \text{if } \hat{s}^2 < \sigma^2 \end{cases} \tag{10}$$

where f equals the Fisher distribution and α the probability level. The redundancy is r for $\hat{s}^2$ and ∞ for σ^2. If the null hypothesis H_0 is accepted, the adjustment can be assumed to be consistent. Otherwise, it requires further investigations [19].

2.4 Development of a stepwise adjustment procedure

Three assumptions are included in the presented adjustment theory of Subsection 2.3:

(i) the order a of the polynomial is known

(ii) no outliers are included in the observations $\mathbf{l}$

(iii) all parameters in the parameter vector $\hat{\mathbf{p}}$ are significant

Nevertheless, an optimal order of the polynomial is not obvious a priori and outliers can be existent inside the observations. An iterative adjustment procedure has therefore to be implemented. This estimates the optimal order a of the polynomial besides the parameters $\hat{\mathbf{p}}$. Furthermore, this procedure has to detect and eliminate outliers due to the assumption of Gaußian distributed measurement errors (see Subsection 2.3).

Outliers can also be included in the datasets. In general, they are due to instable bench marks or mixed up point definitions. Furthermore, they can result from local abnormalities from the general subsidence of ground. Thus, the corresponding observations are not conspicuous in the preadjustment within one epoch but when building the difference between two epochs. Outliers are defined as observations that do not support the general structure of the height changes. This is given if the observation of a point deviates from the polynomial, which fits the observations not being outliers, more than $2.58 \cdot \sigma = 2.58mm$. Here, a confidence interval of 2.58 corresponding to a probability level of 99.0% is chosen [20].

The number $u_{\max}$ of parameters corresponding to the optimal order a (see eq. (2)) is only a maximal limit because not all parameters have to be significant. To guarantee a reliable estimation without an over-parameterization, the number u of significant parameters has to be determined. For the elimination of the non-significant parameters, they are decorrelated by a modified Cholesky-decomposition [25].

Before these steps are processed, the surveying points are transformed because of numerical reasons. First, they are rotated into the main directions by a 2D principal component analysis. Second, they are translated into the centroid and scaled to an interval of $[-1, 1]$. Algorithm 1 shows the final stepwise adjustment procedure. This algorithm is an enhancement of the one already proposed in [34].

It should be emphasized that although Algorithm 1 can estimate the parameters automatically, this algorithm is only a construct that still needs expert knowledge by the user. Especially the evaluation of the detected outliers requires proof of an expert: If the outliers are not distributed randomly in the point cloud, the estimated polynomial cannot be expected to be a good fit of the observations. In this case, the suboptimal determination of the polynomial order could be responsible for the occurence of systematic outliers. To guarantee reliable results, every outlier should be analyzed and the automatic classification as an outlier has always to be questioned. Furthermore, the number of maximal order has to be chosen carefully. In conclusion, there are five requirements that should always be met:

(i) The number of outliers should be small regarding the number of observations

(ii) The number of parameters and the polynomial order should be small regarding the number of observations

(iii) The spatial distribution of outliers should be random

(iv) The estimated residuals should underly a normal distribution

(v) The global test, i.e. H_0, should be accepted

The main results of this algorithm are the estimated significant parameters $\hat{\mathbf{p}}$ and the optimal order. These values are the basis for the presented method for optimization of the network configuration shown in Section 3.

Region A from Figure 1 is parameterized by this algorithm. Figure 2 shows the estimated bivariate polynomial. The polynomial is of order $a = 6$, estimated with $u = 23$ significant parameters. Black crosses indicate the 15 outliers that are detected and eliminated. The redundancy equals $r = 156$ following eq. (9) and $n = 179$.

Algorithm 1: Stepwise adjustment procedure for detection of surface deformations

```
1  Rotate, translate and scale the point cloud
2  Estimation of optimal order
3  Start with order a = 0
4  while H_0 is declined do
5      Estimate parameters p̂ by eq. (5)
6      Calculate residuals v̂ by eq. (7)
7      Elimination of outliers
8      while outliers in data do
9          Eliminate biggest outlier
10         Redo Lines 5–6
11         if outliers are systematic then
12             Go to Line 16
13     Test H_0 by eq. (10)
14     if order is maximal then
15         Go to Line 18
16     Raise order a = a + 1
17 Elimination of parameters
18 Eliminate non-significant parameters
19 Estimation of final parameters
20 Redo Lines 5–10 with original point cloud, fixed order
   and fixed number of parameters
```

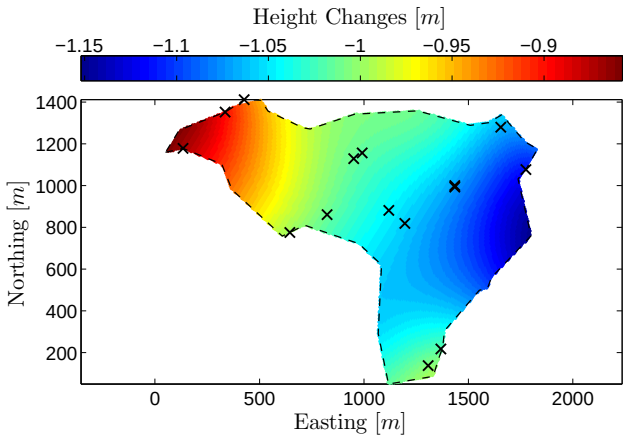

Figure 2. Estimated bivariate polynomial of Region A (epochs 1 – 3, 15 years); black crosses indicate outliers.

3 Strategy for optimization of network configurations

The basic idea of the developed strategy for network optimization consists of three steps:

(i) Building a regular data-adaptive grid to homogenize the spatial surveying point distribution. This increases the relibility of the analysis of surface deformations.

(ii) Network reduction by elimination of individual surveying points if necessary. This increases the economy and cost effectiveness.

(iii) Reinsertion of boundary points. This optional step copes with the bounded expansion of the regions.

Here, two different approaches are combined: First, the sampling theorem known from time series analysis (see Subsection 3.1). This is used to build the data-adaptive regular grid in the first step. Second, impact factors and partial redundancies used in statistics and regression (see Subsection 3.2). They are suitable to verificate the configuration of a network as in the second step. Subsection 3.3 proposes the whole optimization strategy.

3.1 Sampling theorem

In the digital processing of signals, observed waves are transferred by the Fourier transformation from the time domain into the frequency domain. This enables an analysis of the frequencies being enclosed in the observed signal. The sampling theorem used in this context specifies the Nyquist frequency f_N based upon the fixed sampling rate of the observations Δt [1]:

$$f_N = \frac{1}{2\Delta t}. \tag{11}$$

A signal can only be reconstructed from the sampled data if the frequency f of the included waves is less than the Nyquist frequency f_N. Thus, to detect a wave with a frequency of $f = 1Hz$, the sampling rate of the observations has to be $\Delta t < 0.5s$.

This sampling theorem is based upon the assumption of noise-free signals of infinite duration. Therefore, the number of more than 2 observations per wave as indicated by eq. (11) cannot be transferred to empirical data as used in this study. Hence, the number of minimal observations in one wave to detect its frequency should be raised to 5–6 in practial analysis [32]. This guarantees reliability even with noised data of finite observation time.

Consequently, the number of observations needed to reliably detect surface deformations can be calculated. Therefore, the number of waves in the surface deformations has to be known. This will be shown in Subsection 3.3.

3.2 Impact factors and partial redundancies

Observations with high influence can be detetected simply by the knowledge about the geometry of the network without using the actual observations. This leads to the impact factors h_i that are widespread in geodetic analysis [27, 31].

They can be calculated straightforward. Based on the parameter estimation of Subsection 2.3, $\hat{\mathbf{l}} = \mathbf{A}\hat{\mathbf{p}}$ [15] and equation (5) follows

$$\hat{\mathbf{l}} = \underbrace{\mathbf{A}\left(\mathbf{A}^T\mathbf{Q}_{ll}^{-1}\mathbf{A}\right)^{-1}\mathbf{A}^T\mathbf{Q}_{ll}^{-1}}_{\mathbf{H}}\mathbf{l}. \tag{12}$$

Here, $\mathbf{H}$ is called the hat matrix [6]. Its diagonal elements

$$h_i = \mathbf{H}_{i,i} \tag{13}$$

are the impact factors. They describe the influence of every observation l_i on the calculation of the estimated observations $\hat{l}_i$. The values of h_i are in the interval of $0 \leq h_i \leq 1$. An impact factor of $h_i \to 1$ equals a very high impact whereas $h_i \to 0$ equals a negligible impact.

Figure 3 shows the impact factors of Region A: Impact factors are getting higher towards the outer ring of the region. Furthermore, points in sections with low density do have a higher impact than the ones being located in point clusters. The colour is scaled to an interval of $[0.0, 0.4]$ in Figure 3 to stress the distribution. In fact, the highest impact factor is $h_i = 0.93$.

The complement of the impact factor is the partial redundancy r_i

$$r_i = 1 - h_i \tag{14}$$

indicating how one observation is controlled by the others [6, 30]. Both the magnitude as well as the variance of the partial redundancies can be an indicator for the reliablility of the underlying adjustment [28]. Furthermore, partial

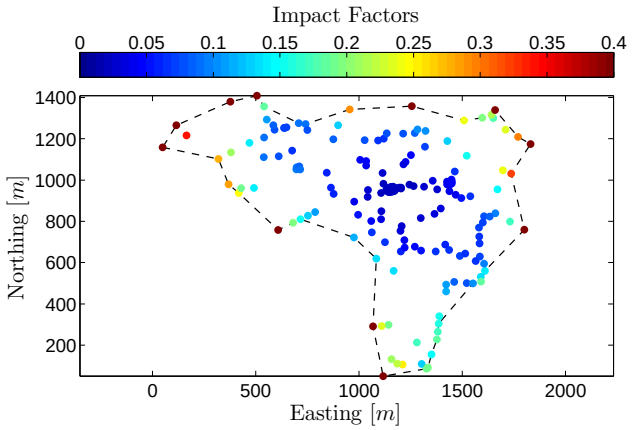

Figure 3. Impact factors h_i of Region A (epochs 1 – 3), the colour is scaled to $[0.0, 0.4]$.

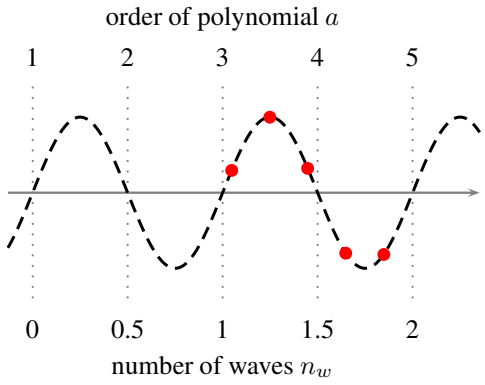

Figure 4. Sketch of a sine curve (black), order a of a polynomial to approximate the sine curve and the corresponding number of waves n_w, regularly spaced surveying points in one wave n_g (red).

redundancies are an indicator for the marginally detectable blunder named as internal reliability [6, 28].

The relative redundancy $\overline{r}$ is a measure for the overall reliability of the network. It is calculated by [6, 12]

$$\overline{r} = \frac{1}{n}\sum_{i=1}^{n} r_i = \frac{r}{n}. \tag{15}$$

This value equals $\overline{r} = 0.87$ for Region A. A verification of the magnitude of relative redundancies in terms of the reliability of a network is given in Section 4.

3.3 Developed strategy for optimization

The strategy for optimization of the network configuration is segmented into three steps. These will be discussed in the following before first results are shown.

3.3.1 Step 1: Building of data-adaptive grid

As soon as the preliminary surface estimation is done, the number of waves of the estimated height changes is known. This can be clarified by Figure 4 where a sine curve is displayed. Furthermore, the order of a polynomial a is shown that is necessary to approximate this sine curve dependent on its length. This relation leads to the connection between the order of a one-dimensional polynomial a and the maximal number of waves n_w that can be approximated by this polynomial:

$$n_w = \frac{a-1}{2}. \tag{16}$$

Assigned to a bivariate polynomial, n_w indicates the number of waves into one coordinate direction. Here, the coordinate system is orientated by the point cloud's principal components as is the case at the parameter estimation (see Subsection 2.4).

Following the sampling theorem (Subsection 3.1), the number of regularly spaced surveying points that are necessary to detect reliably the waves of the polynomial into one direction is thus

$$n_g = \lceil n_w \cdot 5 \rceil . \tag{17}$$

The number of cells in a grid in both planar directions then equals n_g^2. The number of 5 observations per wave is also displayed in Figure 4. This number is chosen because of empirical investigations. Additionally, it fits to the proposed magnitude of 5–6 observations ([32], see Subsection 3.1) being based upon the sampling theorem. This will be verified in Subsection 4.4.

The optimization procedure thus calculates the optimal number of surveying points n_g^2 as well as their optimal position assuming a regular grid. Afterwards, the configuration is optimized as follows: If observations are included in the actual cell, only one of them is necessary for the adjustment of the polynom. The others are rejected. Otherwise, if no observation is contained inside the actual cell, the network is densified by adding an additional observation. The specific location of this new observation inside the cell is rather variable because of the discretization of this approach. Here, it is chosen to be the middle.

The minimal number of waves in eq. (16) is assumed to be 1: $n_w \geq 1$. Otherwise, the transfer of the sampling theorem would not be suitable. Consequently, the minimal number of cells is $n_g^2 = 25$ following eq. (17).

The rejected observations are not required for the estimation of surface deformations due to the optimization procedure. However, they can be regarded as independent control observations as is discussed in the Outlook (Section 5).

3.3.2 Step 2: Data reduction

Under the aspect of economy, the reliability of a geodetic network should not be optimized to infinite magnitude. Rather a defined limit should be reached (see Subsection 1.2). Ideal values for partial redundancies in planar geodetic networks are $0.3 \leq r_i \leq 0.7$ [29]. An observation having a partial redundancy of $r_i > 0.7$ can thus be eliminated, whereas one with $r_i < 0.3$ should be supported by additional observations.

Thus, points having a high partial redundancy after the first optimization step are iteratively eliminated. This data reduction step is widespread [8, 24]. The threshold is set up as $r_i \leq 0.95$. This may seem to be very high in comparison to the interval of $0.3 \leq r_i \leq 0.7$ for planar networks but it will be verified later in Subsection 4.4.

3.3.3 Step 3: Reinsertion of boundary points

The optional third step reinserts boundary points. This step is not essential following the previous efforts to build up a constant grid of surveying points. Nevertheless, this step counteracts two difficulties:

(i) Boundary points have a high impact using polynomials (see Figure 3).

(ii) The sampling theorem assumes signals of infinite expansion (see Subsection 3.1). This is not fulfilled because of the limited size of the regions in this study.

Because of these two difficulties, boundary points are important to guarantee reliable estimates. Hence, it is reasonable not to reject any boundary points. However, to highlight the benefit of the first two steps, this third step is excluded in the following analysis.

3.3.4 Resulting algorithm

Algorithm 2 presents the resulting strategy for optimization of the network configuration. This approach is based upon the theory of time series analysis (sampling theorem) and statistics (partial redundancies). Two values, which are verified in Subsection 4.4, are set empirically:

(i) The number of 5 observations per wave (eq. (17))

(ii) The threshold of $r_i \leq 0.95$ for the maximal partial redundancy that is not rejected

Figure 5 shows the optimization of the configuration of Region A. The order of the polynomial is $a = 6$, the number of waves is $n_w = 2.5$ and the number of grid points in each of both directions is $n_g = 13$ (see eqs. (16) and (17)). 106 observations (of 179) have been rejected so that 73 observations of the original point cloud remain. 12 observations are added so that the number of surveying points of this region with an optimal configuration is $n_{opt} = 85$.

Algorithm 2: Optimization of network configuration

```
1  Estimate polynomial by Algorithm 1
2  1. Building of data-adaptive grid
3  Calculate number of waves n_w by eq. (16)
4  Build regular grid with n_g^2 cells by eq. (17)
5  for j = 1 to number of cells do
6      if cell(j) is empty then
7          Add point in middle of cell
8      else if cell(j) is filled then
9          Accept point that is nearest to the middle
10         Reject the others
11 2. Data reduction
12 for i = 1 to number of points do
13     Calculate partial redundancies r_i by eq. (14)
14     if max(r_i) > 0.95 then
15         Reject point with max(r_i)
16     else
17         Go to Line 19
18 3. Reinsertion of boundary points (optional)
19 for j = 1 to number of boundary points do
20     if boundary point (j) ∉ point cloud then
21         Reinsert boundary point (j)
```

Region A should thus be densified at 12 cells whereas 106 surveying points could be rejected. Consequently, an optimization of the network configuration could be performed to raise the reliability of the analysis in the whole region.

4 Verification of the developed strategy

Various test regions are used to verify Algorithm 2. The objective analysis that can be achieved regarding the optimal number of points n_{opt} and the resulting relative redundancy $\overline{r}_{opt}$ is pointed out.

4.1 Verification of Region A

Region A is optimized based on the proposed strategy. Before the optimization, its relative redundancy was $\overline{r} = 0.87$ (see Subsection 3.2). This values equals $\overline{r}_{opt} = 0.73$ after the optimization. This is close to the upper end of the interval $0.3 \leq r_i \leq 0.7$ of partial redundancies usually demanded in planar geodetic networks (see Subsection 1.2).

Figure 6 shows the impact factors of Region A after optimization revealing two facts: (1) The mean value of the impact factors is increased (the mean value of the partial redundancies is decreased, as is already mentioned by $\overline{r}_{opt}$).

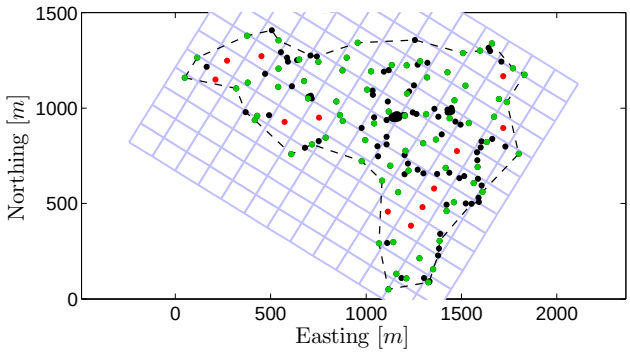

Figure 5. Optimization of Region A (epochs 1 – 3, 15 years); rejected points (black), accepted points (green), added points (red) and underlying grid cells (blue).

(2) The distribution of the impact factors is more homogeneous. The general increase of impact factors towards the border of the region is due to the fact that polynomials are less reliable there.

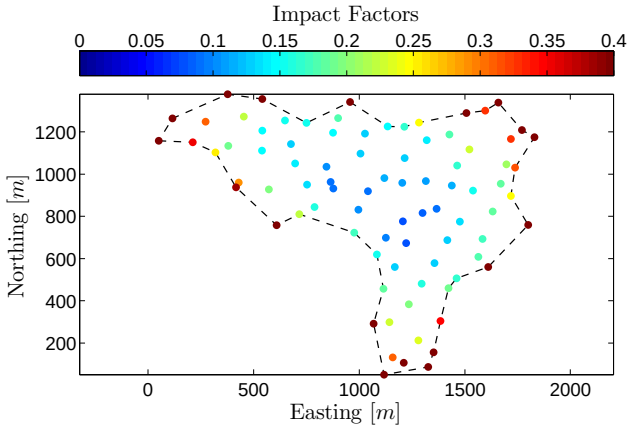

Figure 6. Impact factors h_i of Region A (epochs 1 – 3) after optimization, the colour is scaled to $[0.0, 0.4]$.

Until now, the height changes between epochs 1 – 3 have been analyzed. In epoch 2, the network configuration has been optimized without using Algorithm 2. An analysis of the densified network between epochs 2 – 3 is thus reasonable. Figure 7 shows the optimization of the improved network. Here, the order of the approximated polynomial, the number of waves and the number of grid points remain as in Figure 5 ($a = 6$, $n_w = 2.5$, $n_g = 13$).

The densification of the network at epoch 2 to a number of $n = 635$ observations (441 additional points) did benefit the configuration only partially. Instead of 12 surveying points that should be added between epochs 1 – 3, now 9 observations should be added regarding Algorithm 2. This is because the densification was performed not homogeneously but along the courses of streets. Thus, some sections of the region are still not covered optimally. The relative redundancy was $\overline{r} = 0.96$ before the optimization with $u = 23$ parameters. After the optimization, this equals $\overline{r}_{opt} = 0.76$. Again, this value is near the desired interval.

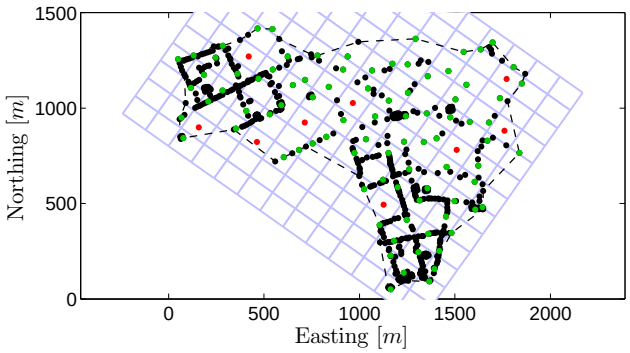

Figure 7. Optimization of Region A (epochs 2 – 3, 8 years); rejected points (black), accepted points (green), added points (red) and underlying grid cells (blue).

4.2 Verification of Region B

Region B also consists of 3 epochs of levelling. Figure 8 shows its optimization concerning epochs 1 – 2: The $n = 267$ observations are nearly sufficient for a reliable adjustment ($a = 4$, $u = 12$), only one observation should be added. Furthermore, the point cloud could be thinned out to a number of $n_{opt} = 42$. This leads to a relative redundancy of $\overline{r} = 0.96$ before and $\overline{r}_{opt} = 0.71$ after the optimization.

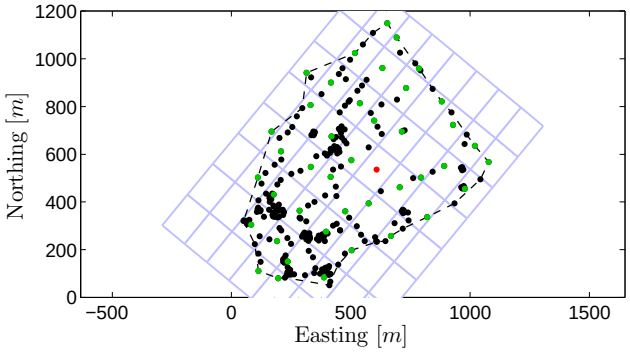

Figure 8. Optimization of Region B (epochs 1 – 2, 8 years); rejected points (black), accepted points (green), added points (red) and underlying grid cells (blue).

Figure 9 illustrates the surveying points and the optimization regarding the first and third epoch ($n = 155$, $a = 4$, $u = 13$). Because the time between the epochs is 12 years now, less identical surveying points are covered. However, the fewer observations are still sufficient for a reliable adjustment. Only one more observation is missing than in the first period while many observations are still rejected. The relative redundancy has been $\overline{r} = 0.92$ before the optimization and is $\overline{r}_{opt} = 0.69$ afterwards.

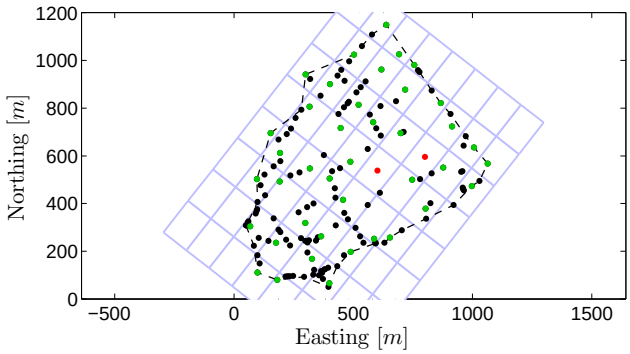

Figure 9. Optimization of Region B (epochs 1 – 3, 12 years); rejected points (black), accepted points (green), added points (red) and underlying grid cells (blue).

4.3 Verification of Region C

Figure 10 reveals the configuration optimization of Region C, epochs 1 – 2. A big cluster of points is located in the north. Thus, the observations especially in the south would have a very low impact on the parameter estimation based on this configuration (if all observations are equally weighted, as assumed here). The optimization upgrades the configuration so that the different sectors of the region contribute in similar parts to the parameter estimation. Because of the locally bounded point cluster, only 37 of the $n = 136$ points are necessary ($a = 4$, $u = 11$) while 6 new points have been added. This leads to $n_{opt} = 43$. Furthermore, the relative redundancy is reduced from $\overline{r} = 0.92$ to $\overline{r}_{opt} = 0.74$.

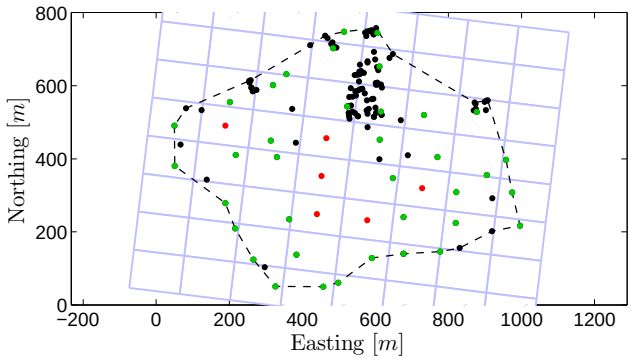

Figure 10. Optimization of Region C (epochs 1 – 2, 7 years); rejected points (black), accepted points (green), added points (red) and underlying grid cells (blue).

Here, also a network densification was performed after epoch 1. Regarding the configuration optimization of epochs 2 – 3 (Figure 11), two main aspects can be observed:

(i) Even though the order of the polynomial has risen to $a = 5$, the number of significant parameters remains constant at $u = 11$. This leads to a relative redundancy of $\overline{r}_{opt} = 0.83$ after optimization. This is higher than the ones of the proposed regions until now.

(ii) Eight grid cells (highlighted in yellow) do not contain any observation in the optimized configuration. These observations are rejected in the data reduction step due to partial redundancies of $r_i > 0.95$.

Both these findings are due to Algorithm 2: Only the order a of the polynomial is considered as criterion for the number of grid cells n_g^2 but not the number of parameters u. In contrast, the partial redundancies r_i and the relative redundancy $\overline{r}$ only depend on the number of paramters u, not on the order of the polynomial a.

Hence, the proposed method in Algorithm 2 is limited to the assumption that the order a and the number of significant parameters u are proportional. This is only the case if almost all parameters are significant. If even all parameters are significant, eq. (2) describes this proportion. However, the two specified thresholds could be readjusted to overcome this limiation.

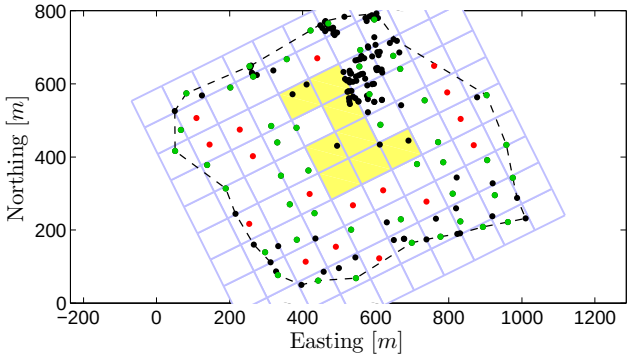

Figure 11. Optimization of Region C (epochs 2 – 3, 10 years); rejected points (black), accepted points (green), added points (red) and underlying grid cells (blue); cells not containing points in the optimized configuration are yellow.

4.4 Final results

Table 1 summarizes the results of the previous subsections. The relative redundancies $\overline{r}_{opt}$ are all in the interval of $0.69 \leq \overline{r}_{opt} \leq 0.76$ after the optimizations. The higher relative redundancy of Region C (epochs 2–3, see Subsection 4.3) indicates the limitation of the proposed method.

Although the threshold of $r_i > 0.95$ for rejecting observations seems to be very high, the relative redundancies $\overline{r}_{opt}$ are near the interval of $0.3 \leq r_i \leq 0.7$, proposed as desired in planar networks [29]. The fact that they are slightly higher than this interval should not imply that the configuration is still too dense. This would mean that the threshold of 5 observations per wave should be reduced.

region	epochs	a	u	n	$\overline{r}$	n_{opt}	$\overline{r}_{opt}$
A	1–3	6	23	179	0.87	85	0.73
	2–3	6	23	635	0.96	97	0.76
B	1–2	4	12	267	0.96	42	0.71
	1–3	4	13	155	0.92	42	0.69
C	1–2	4	11	136	0.92	43	0.74
	2–3	5	11	168	0.93	64	0.83

Table 1. Parameters describing the network configurations and the approximated polynomials; a: order of polynomial; u: number of significant parameters; n (n_{opt}): number of observations (after optimization); $\overline{r}$ ($\overline{r}_{opt}$): relative redundancy (after optimization).

It is rather the fact that the proposed interval is not completely transferable to the application discussed here. The proposed interval considers planar networks, where station coordinates are estimated. Since the present study aims at continuously parameterizing surface deformations, higher partial redundancies than usual should be achieved. Relative redundancies of $\overline{r} \approx 0.75$ with observations being distributed equably over the region are therefore still recommendable for the present study – even considering cost effectiveness. In conclusion, Algorithm 2 objectively optimizes the configuration of a given height network.

5 Discussion and outlook

This study presents an algorithm that handles the third order design of height networks. This has not been solved satisfactorily based on the discussed literature. The proposed method analyzes a given height network concerning its configuration. Therefore, it estimates the optimal number of surveying points that should be used to guarantee a reliable estimation of the underlying bivariate polynomial. Furthermore, the method

- recommends the rejection or acceptance of the already given observations and
- places additional surveying points at positions where they are needed in terms of an optimal configuration.

Here, the sampling theorem from time series analysis and the partial redundancies known in statistics are combined. The first one is based on the order of the polynomial, the latter one on the number of parameters. Two empirically set thresholds are integrated to specifiy the density of the resulting optimized configuration.

The proposed algorithm has one limitation: The order of the polynomial and the number of its significant parameters are assumed to be proportional. If this is not fulfilled, the resulting optimized configuration might still be too dense. Then, the two included thresholds need to be readjusted. This should again lead to a network configuration that equals a regular grid of surveying points.

The optimization procedure is verified by several test regions. The following benefits can be achieved:

- The observations that are rejected by the optimization procedure can be regarded as independent control observations. These control observations could be used to support and verify the adjustment because they would not take part in the parameter estimation.
- The relative redundancy of the optimized point cloud $\overline{r}_{opt}$ is more meaningful than the original one ($\overline{r}$). This is because the spatial distribution of the given surveying points might be very inhomogeneous. A high relative redundancy $\overline{r}$ could misleadingly imply that the observations are reliable even in sections where surveying points are given only sparsely.
- Other important parameters describing the reliability of a geodetic network are improved: The internal reliability (marginally detectable blunder) and the external reliability (impact of outliers onto the estimated parameters) [6, 12, 30].

It should be emphasized that the proposed method alters the configuration to guarantee optimal reliability. A given suboptimal configuration does not automatically mean that the detection of surface deformations is impossible; the parameter estimation is simply not optimal.

Generally, polynomials have one disadvantage – the increase of impact of observations lying on the outer ring of the observed region (see Figure 3). A strategy to overcome this drawback is the reinsertion of boundary points as mentioned in Subsection 3.3. Furthermore, twin points could be introduced. These twin points could be positioned in the direct neighbourhood of the already observed surveying points lying on the outer ring of the region. Hence, the partial redundancies would be enhanced significantly at the borders of the region. This procedure would even be reasonable regarding the economy: The installation and levelling of additional points in the direct neighbourhood of already existing ones is neither time-consuming nor cost-intensive. These aspects have to be studied further.

References

[1] M. Bellanger, *Digital Processing of Signals*, 2nd ed, John Wiley & Sons, Chichester, New York, Brisbane, Toronto, Singapore, 1989.

[2] S. Chatterjee and A. S. Hadi, Influential observations, high leverage points, and outliers in linear regression, *Statistical Science* **1** (1986), 379–416.

[3] R. D. Cook, Detection of influential observation in linear regression, *Technometrics* **19** (1977), 15–18.

[4] R. D. Cook, Influential observations in linear regression, *J Am Stat Assoc* **74** (1979), 169–174.

[5] Q. Dalmolin and R. Oliveira, Inverse eigenvalue problem applied to weight optimisation in a geodetic network, *Survey Review* **43** (2011), 187–198.

[6] W. Förstner, Reliability analysis of parameter estimation in linear models with applications to mensuration problems in computer vision, *Comput Vision Graph* **40** (1987), 273–310.

[7] E. W. Grafarend, *Third-order design of geodetic networks*, Optimization of Design and Computation of Control Networks (F. Halmos and J. Somogyi, eds.), Akadémiai Kiadó, Budapest, 1979, pp. 133–149.

[8] L. Gründig and J. Bahndorf, *Optimale Planung und Analyse von 2- und 3-dimensionalen geodätischen Netzen im Ingenieurbereich - Programmsystems OPTUN*, Beiträge zum IX. Internationalen Kurs für Ingenieurvermessung (Rinner, Schelling and Brandstätter, eds.), Dümmler, Bonn, 1984.

[9] J. G. Hayes and J. Halliday, The least-squares fitting of cubic spline surfaces to general data sets, *J Inst Maths Applics* **14** (1974), 89–103.

[10] R. Hsu, Precomputing influences of observation for a network, *J Appl Geodesy* **126** (2000), 8–17.

[11] M. Illner, *Anlage und Optimierung von Verdichtungsnetzen*, Ph.D. thesis, University of Karlsruhe, 1986, DGK C 317.

[12] M. Kavouras, *On the detection of outliers and the determination of reliability in geodetic networks*, Department of Geodesy and Geomatics Engineering, University of New Brunswick, Report no. 87, 1982.

[13] R. Kelm, *Graph methods within the optimal design of geodetic nets*, Optimization of Design and Computation of Control Networks (F. Halmos and J. Somogyi, eds.), Akadémiai Kiadó, Budapest, 1979, pp. 151–162.

[14] K.-R. Koch, Optimization of the configuration of geodetic networks, in: *Proceedings of the International Symposium on Geodetic Networks and Computations of the International Association of Geodesy* (R. Sigl, ed.), III: Optimal Design of Geodetic Networks, pp. 82–89, Munich, August 31 – September 5 1981 1982.

[15] K.-R. Koch, *Parameter Estimation and Hypothesis Testing in Linear Models*, Springer, Berlin, Heidelberg, New York, 1988.

[16] T. Lahmer, Optimal experimental design for nonlinear ill-posed problems applied to gravity dams, *Journal of Inverse Problems* **27** (2011).

[17] P. Lancaster and K. Salkauskas, *Curve and surface fitting - an introduction*, Academic Press LTD., London, 1986.

[18] C. Léger and N. Altman, Assessing influence in variable selection problems, *J Am Stat Assoc* **88** (1993), 547–556.

[19] E. M. Mikhail and F. Ackermann, *Observations and least squares*, Dun-Donelly, New York, 1976.

[20] Normenausschuss Bauwesen im DIN, *Part 4: Adjustment of observations and statistics*, DIN 18709: Concepts, abbreviations and symbols in geodesy, Beuth, Berlin, 2010.

[21] A. Nuckelt, *Dreidimensionale Plattenkinematik: Strainanalyse auf B-Spline-Approximationsflächen am Beispiel der Vrancea-Zone / Rumänien*, Ph.D. thesis, University of Karlsruhe, 2007, Schriftenreihe des Studiengangs Geodäsie und Geoinformatik 2007,5.

[22] D. Pena, A new statistic for influence in linear regression, *Technometrics* **47** (2005), 1–12.

[23] G. Schmitt, *Review of network designs: criteria, risk functions, design ordering*, Optimization and Design of Geodetic Networks (E. W. Grafarend and F. Sansò, eds.), Springer, Berlin, Heidelberg, New York, Tokyo, 1985, pp. 6–10.

[24] G. Schmitt, *Third order design*, Optimization and Design of Geodetic Networks (E. W. Grafarend and F. Sansò, eds.), Springer, Berlin, Heidelberg, New York, Tokyo, 1985, pp. 122–131.

[25] P. Schwintzer, *Zur Bestimmung der signifikanten Parameter in Approximationsfunktionen*, Beiträge aus dem Institut für Geodäsie der UniBW München, 10, Caspary and Schödlbauer and Welsch, 1984, pp. 71–91.

[26] A. A. Seemkooei, *Analytical methods in optimization and design of geodetic networks*, Ph.D. thesis, Department of Surveying Engineering, K. N. Toosi University of Technology Tehran, Iran, 1998.

[27] A. A. Seemkooei, Comparison of reliability and geometrical strength criteria in geodetic networks, *J Geod* **75** (2001), 227–233.

[28] A. S. Silva, H. L Baiao and V. M. C. Romao, Software to optimize surveying networks, in: *13th FIG Symposium on Deformation Measurement and Analysis; 4th IAG Symposium on Geodesy for Getechnical ans Structural Engineering*, Lisbon, May 12–15 2007.

[29] M. Staudinger, *A cost orientated approach to geodetic network optimisation*, Ph.D. thesis, Faculty of Technical Science, University of Technology, Vienna, 1999.

[30] P. J. G. Teunissen, *Optimization and Design of Geodetic Networks*, Quality control in geodetic networks (E. W. Grafarend and F. Sansò, eds.), Springer, Berlin, Heidelberg, New York, Tokyo, 1985, pp. 526–547.

[31] M. Vennebusch, A. Nothnagel and H. Kutterer, Singular value decomposition and cluster analysis as regression diagnostics tools for geodetic applications, *J Geod* **83** (2009), 877–891.

[32] W. Welsch, O. Heunecke and H. Kuhlmann, *Auswertung geodätischer Überwachungsmessungen*, Handbuch Ingenieurgeodäsie (M. Möser, G. Müller, H. Schlemmer and H. Werner, eds.), Wichmann, Heidelberg, 2000.

[33] O. Wälder, *Spezielle Verfahren zur Analyse von raumbezogenen Daten*, Ph.D. thesis, TU Dresden, 2008, DGK C 625.

[34] P. Zeimetz and H. Kuhlmann, Use of parametric models for analyzing ground movement measurements in the Rhenish lignite mining area, *World of Mining - Surface & Underground* **5** (2011), 256–264.